

# Fluorescence Probing of Interior, Interfacial, and Exterior Regions in Solution Aggregates of Poly(ethylene oxide)–Poly(propylene oxide)–Poly(ethylene oxide) Triblock Copolymers

Christian D. Grant, Michelle R. DeRitter,<sup>†</sup> Karen E. Steege,<sup>‡</sup>  
Tatiana A. Fadeeva, and Edward W. Castner, Jr.\*

Department of Chemistry and Chemical Biology, Rutgers, The State University of New Jersey,  
610 Taylor Road, Piscataway, New Jersey 08854-8087

Received October 1, 2004. In Final Form: November 22, 2004

Fluorescence spectroscopy is used to probe local environments within regions of different polarity and hydrophobicity in aqueous aggregates of PEO<sub>109</sub>–PPO<sub>41</sub>–PEO<sub>109</sub> triblock copolymers. These copolymer aggregates have well characterized microphases in aqueous solution. Concentrations and temperatures for our studies are chosen such that the copolymers are in unimer, micellar, or micellar hydrogel forms. The observed fluorescence spectra and lifetimes from solutions individually labeled with each of the three coumarin probes report on the changes in the local polarity of the core, exterior, interfacial, and corona regions of these copolymer aggregates. This multiple fluorescence probe methodology will be straightforward to apply in general to problems in polymer and biopolymer aggregates, especially those that display strong hydrophobic effects.

## Introduction

Complex aqueous aggregates such as micelles, biopolymers, vesicles, and hydrogels show substantial variations in local properties throughout different regions of the aggregate.<sup>1–4</sup> Local intermolecular interactions vary greatly, ranging from strongly hydrophobic and reduced polarity regions lacking water to strongly polar and hydrogen-bonding environments (in water rich regions).<sup>5–7</sup> We present results using three coumarin fluorescence probes of greatly differing hydrophobicity and show how different aggregate regions can be independently probed using static and time-resolved fluorescence spectroscopy. Using A–B–A triblock copolymers as a model system, we obtain detailed information on the variations in local interactions and dynamics between regions with different hydrophobicity.

Symmetric (A–B–A) triblock copolymers of poly(ethylene oxide)–poly(propylene oxide)–poly(ethylene oxide) (PEO–PPO–PEO) are nonionic, high molecular weight surfactants that have unique and interesting properties.<sup>4</sup> They are widely available from several manufacturers (including BASF, Dow, ICI, and Serva) and have broad industrial uses including foaming and detergent applications, lubrication, and emulsification. Because of their low toxicity and amphiphilic nature, they

have also been utilized as controlled drug encapsulation and delivery systems.<sup>8–10</sup>

PEO–PPO–PEO triblock copolymers show interesting and complex aqueous solution behavior.<sup>4</sup> As many as nine phases can be identified as concentration and/or temperature are varied. These microphases include unimers, spherical and rodlike micelles, several types of liquid crystals, cubic or hexagonally packed hydrogels, and lamellar aggregates.<sup>11–13</sup> Typically these systems present a temperature-dependent microphase transition from unimers to micelles in the concentration range from 1 to 10 wt %.

Though many PEO and PPO chain lengths are available, we chose to study the PEO<sub>109</sub>–PPO<sub>41</sub>–PEO<sub>109</sub> triblock copolymer (BASF Pluronic F88). Our primary motivation for this choice is that by varying Pluronic F88 concentrations, we obtain a wide range of distinct solution types, including unimers, micelles, and hydrogels. The aggregation properties of Pluronic F88 have been widely characterized.<sup>14–18</sup> A schematic illustrating the different types of structures (random coil unimers, micelles, and cubic packed hydrogels) that PEO–PPO–PEO can form in

<sup>†</sup> Present address: Department of Chemistry, University of Pennsylvania, 231 South 34th Street, Philadelphia, PA 19104-6323.

<sup>‡</sup> NSF IGERT trainee in Biointerfacial Engineering.

(1) Jönsson, B.; Lindman, B.; Holmberg, K.; Kronberg, B. *Surfactants and polymers in aqueous solution*; John Wiley & Sons: New York, 1998.

(2) Israelachvili, J. N. *Intermolecular and surface forces*, 2nd ed.; Academic Press: San Diego, 1991.

(3) Evans, D. F.; Wennerström, H. *The colloidal domain: Where physics, chemistry, biology, and technology meet*, 2nd ed.; Wiley-VCH: New York, 1999.

(4) Alexandridis, P.; Hatton, T. A. *Colloids Surf.*, A **1995**, *96*, 1.

(5) Levinger, N. E. *Curr. Opin. Colloid Interface Sci.* **2000**, *5*, 118.

(6) Nandi, N.; Bhattacharyya, K.; Bagchi, B. *Chem. Rev.* **2000**, *100*, 2013.

(7) Bhattacharyya, K.; Bagchi, B. *J. Phys. Chem. A* **2000**, *104*, 10603.

(8) Kabanov, A. V.; Nazarova, I. R.; Astafieva, I. V.; Batrakova, E. V.; Alakhov, V. Y.; Yaroslavov, A. A.; Kabanov, V. A. *Macromolecules* **1995**, *28*, 2303.

(9) Scherlund, M.; Welin-Berger, K.; Brodin, A.; Malmsten, M. *Eur. J. Pharm. Sci.* **2001**, *14*, 53.

(10) Rapoport, N. Y.; Herron, J. N.; Pitt, W. G.; Pitina, L. *J. Controlled Release* **1999**, *58*, 153.

(11) Alexandridis, P.; Olsson, U.; Lindman, B. *Langmuir* **1998**, *14*, 2627.

(12) Schillen, K.; Brown, W.; Johnsen, R. M. *Macromolecules* **1994**, *27*, 4825.

(13) Wanka, G.; Hoffmann, H.; Ulbricht, W. *Macromolecules* **1994**, *27*, 4145.

(14) Brown, W.; Schillen, K.; Hvidt, S. *J. Phys. Chem.* **1992**, *96*, 6038.

(15) Yu, G.; Altinok, H.; Nixon, S. K.; Booth, C.; Alexandridis, P.; Hatton, T. A. *Eur. Polym. J.* **1997**, *33*, 673.

(16) Jain, N. J.; Aswal, V. K.; Goyal, P. S.; Bahadur, P. *J. Phys. Chem. B* **1998**, *102*, 8452.

(17) Guo, C.; Wang, J.; Liu, H.-z.; Chen, J.-y. *Langmuir* **1999**, *15*, 2703.

(18) Aswal, V. K.; Goyal, P. S.; Kohlbrecher, J.; Bahadur, P. *Chem. Phys. Lett.* **2001**, *349*, 458.

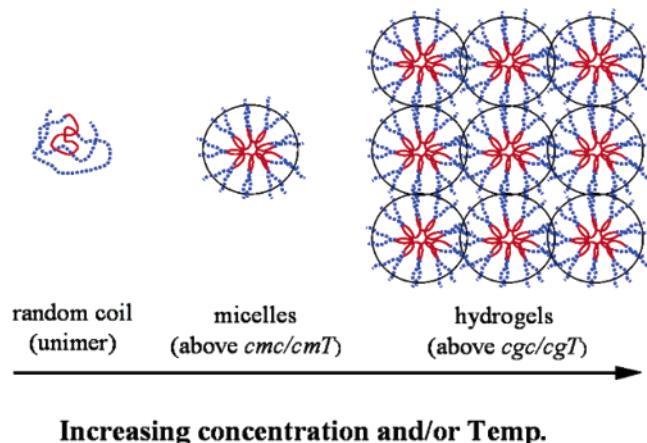


**Figure 1.** Schematic of random coil unimer, micelle, and face-centered cubic gel phases of aqueous F88 triblock copolymer solutions.

aqueous solution is shown in Figure 1.<sup>19</sup> The 5 w/v% aqueous F88 copolymer solution undergoes a microphase transition from unimers to micelles at  $\sim 35$  °C, while the microphase transition for the 25 w/v% F88 solution is found at  $\sim 22$  °C, with macroscopic hydrogelation occurring at about 40 °C.

The unimer to micelle microphase transition in the PEO–PPO–PEO triblock copolymer systems is driven by the hydrophobic effect, via the same dehydration mechanism by which some aqueous polymers and proteins precipitate with increasing temperature.<sup>20</sup> Although poly(propylene oxide) is often thought to be hydrophobic and water insoluble, it is in fact somewhat soluble for low temperatures in the 2–15 °C range, with a precipitation cloud point that occurs between 15 and 30 °C for increasing PPO chain lengths.<sup>21</sup> For a fixed copolymer concentration, entropy favors the release of hydrogen-bonded waters in the PPO core with increasing temperature. Dehydration of the central poly(propylene oxide) block of the copolymer drives unimer aggregation to form micelles. The hydrophobic PPO blocks comprise the core, and the PEO blocks form the hydrated exterior or corona. Micellization in these systems, a consequence of PPO block dehydration, has been extensively studied via several techniques including small angle neutron scattering (SANS),<sup>16,18,22–24</sup> dynamic light scattering (DLS),<sup>15,25,26</sup> differential scanning calorimetry (DSC),<sup>13,27–29</sup> Fourier transform Raman and infrared spectroscopies,<sup>17</sup> and fluorescence spectroscopy.<sup>26,30–32</sup>

At higher concentrations of Pluronic solutions, micelle–micelle entanglement (PEO interpenetrating between micelles) leads to solution gelation with increasing tem-

perature.<sup>4,14,21,33,34</sup> These triblock copolymer hydrogels have been characterized by the methods cited above and also by NMR dynamics.<sup>35,36</sup> At high enough temperatures, the gel melts due to micellar structural changes, such as spherical micelles becoming rodlike micelles,<sup>12</sup> and then eventually the cloud point is reached as PEO chains fully dehydrate to finally form two macrophases. The 25 w/v% aqueous F88 solutions can gel at elevated temperatures ( $\sim 40$  °C) because the micelle volume fraction reaches the critical value of 0.57 for cubic packed spheres. However, the 5 w/v% aqueous solutions lack sufficient micelle volume fraction to form hydrogels.

Several species of Pluronic and related PEO–PPO–PEO triblock copolymers have previously been investigated using fluorescence spectroscopy.<sup>8,26,30–32,37–39</sup> Almgren and co-workers determined the aggregation number for Pluronic triblock copolymer micelles using the pyrene quenching method.<sup>37</sup> Alexandridis et al. used the pyrene solvent polarity indicator scale to determine the effective polarity inside Pluronic micelle cores.<sup>26</sup> Nivaggioli et al. used pyrene to determine the polarity of a fixed concentration of Pluronic micellar solution as a function of temperature;<sup>26</sup> their results for five different Pluronic copolymers are qualitatively very similar to what we observe in our Pluronic F88 samples for the hydrophobic C153 probe molecule. Kabanov et al. used two very hydrophobic probes, pyrene and diphenylhexatriene (DPH), to examine partitioning of fluorescence probes between different microphases.<sup>8</sup> Jeon et al. used the rhodamine 123 cation to probe the viscosity of the exterior water phase in 20 wt % Pluronic F127 hydrogels using fluorescence anisotropy measurements<sup>32</sup> and found that though the samples became solid, the local microviscosity sensed by the probe was waterlike, which agrees with the C343/Na<sup>+</sup> results presented below.

Environments of varying complexity can be probed by choosing the appropriate solvatochromic probe molecules. For many recent studies, 7-aminocoumarins have been shown to be excellent probes of solvation dynamics and local friction.<sup>40,41</sup> These coumarin molecules have been used for probing complex environments including polymers,<sup>42,43</sup> reverse<sup>44–51</sup> and normal<sup>52,53</sup> micelles, sol–gels,<sup>54</sup>

(30) Nivaggioli, T.; Alexandridis, P.; Hatton, T. A.; Yekta, A.; Winnik, M. A. *Langmuir* **1995**, *11*, 730.

(31) Nivaggioli, T.; Tsao, B.; Alexandridis, P.; Hatton, T. A. *Langmuir* **1995**, *11*, 119.

(32) Jeon, S.; Granick, S.; Kwon, K. W.; Char, K. *J. Polym. Sci., Part B: Polym. Phys.* **2002**, *40*, 2883.

(33) Mortensen, K.; Brown, W.; Norden, B. *Phys. Rev. Lett.* **1992**, *68*, 2340.

(34) Mortensen, K.; Brown, W. *Macromolecules* **1993**, *26*, 4128.

(35) Walderhaug, H.; Nystroem, B. *J. Phys. Chem. B* **1997**, *101*, 1524.

(36) Walderhaug, H. *J. Phys. Chem. B* **1999**, *103*, 3352.

(37) Almgren, M.; Bahadur, P.; Jansson, M.; Li, P.; Brown, W.; Bahadur, A. *J. Colloid Interface Sci.* **1992**, *151*, 157.

(38) Kositzka, M. J.; Bohne, C.; Alexandridis, P.; Hatton, T. A.; Holzwarth, J. F. *Macromolecules* **1999**, *32*, 5539.

(39) Nakashima, K.; Takeuchi, K. *Appl. Spectrosc.* **2001**, *55*, 1237.

(40) Horng, M. L.; Gardecki, J. A.; Papazyan, A.; Maroncelli, M. *J. Phys. Chem.* **1995**, *99*, 17311.

(41) Horng, M. L.; Gardecki, J. A.; Maroncelli, M. *J. Phys. Chem. A* **1997**, *101*, 1030.

(42) Argaman, R.; Huppert, D. *J. Phys. Chem. A* **1998**, *102*, 6215.

(43) Shirota, H.; Segawa, H. *J. Phys. Chem. A* **2003**, *107*, 3719.

(44) Pant, D.; Riter, R. E.; Levinger, N. E. *J. Chem. Phys.* **1998**, *109*, 9995.

(45) Riter, R. E.; Willard, D. M.; Levinger, N. E. *J. Phys. Chem. B* **1998**, *102*, 2705.

(46) Riter, R. E.; Undiks, E. P.; Levinger, N. E. *J. Am. Chem. Soc.* **1998**, *120*, 6062.

(47) Riter, R. E.; Undiks, E. P.; Kimmel, J. R.; Levinger, N. E. *J. Phys. Chem. B* **1998**, *102*, 7931.

(48) Willard, D. M.; Riter, R. E.; Levinger, N. E. *J. Am. Chem. Soc.* **1998**, *120*, 4151.

(49) Pant, D.; Levinger, N. E. *Langmuir* **2000**, *16*, 10123.

(19) Prudhomme, R. K.; Wu, G. W.; Schneider, D. K. *Langmuir* **1996**, *12*, 4651.

(20) Creighton, T. E. *Proteins: Structures and molecular properties*, 2nd ed.; W. H. Freeman: New York, 1993.

(21) Mortensen, K. *J. Phys.: Condens. Matter* **1996**, *8*, A103.

(22) Mortensen, K.; Pedersen, J. S. *Macromolecules* **1993**, *26*, 805.

(23) Goldmints, I.; vonGottberg, F. K.; Smith, K. A.; Hatton, T. A. *Langmuir* **1997**, *13*, 3659.

(24) Goldmints, I.; Yu, G. E.; Booth, C.; Smith, K. A.; Hatton, T. A. *Langmuir* **1999**, *15*, 1651.

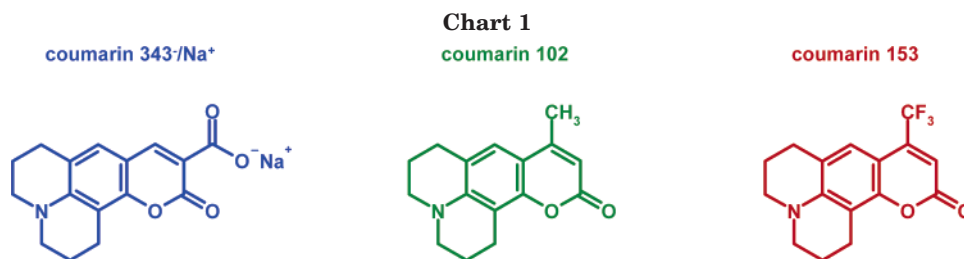
(25) Brown, W.; Schillen, K.; Almgren, M.; Hvidt, S.; Bahadur, P. *J. Phys. Chem.* **1991**, *95*, 1850.

(26) Alexandridis, P.; Nivaggioli, T.; Hatton, T. A. *Langmuir* **1995**, *11*, 1468.

(27) Alexandridis, P.; Holzwarth, J. F.; Hatton, T. A. *Macromolecules* **1994**, *27*, 2414.

(28) Armstrong, J.; Chowdhry, B.; Mitchell, J.; Beezer, A.; Leharne, S. *J. Phys. Chem.* **1996**, *100*, 1738.

(29) Wanka, G.; Hoffmann, H.; Ulbricht, W. *Colloid Polym. Sci.* **1990**, *268*, 101.



vesicles,<sup>5</sup> proteins,<sup>55</sup> cyclodextrins,<sup>56</sup> molten salts,<sup>57</sup> zeolites,<sup>58</sup> drug-delivery polymers,<sup>59</sup> and room-temperature ionic liquids.<sup>60–64</sup> Recently Shirota et al. studied the fluorescence dynamics of C102 and C153 inside SDS micelles.<sup>65</sup> In this work, the same qualitative results were obtained for both probes in the SDS micelle interiors,<sup>65</sup> as the range of environments in which the hydrophobic probe molecules can partition is not so heterogeneous as in the present case of the triblock copolymer aqueous aggregates.

It is important to characterize the solution properties of aqueous polymer aggregates by multiple experimental methods, since these complex systems are highly sensitive to additional (impurity) components in solution, e.g., salts, homopolymers, and surfactants.<sup>16,28,37,66</sup> To this end, we use several techniques to characterize the Pluronic F88 aqueous solutions, including DSC and DLS, for determining both macroscopic and microscopic properties, respectively. As these other solution properties are characterized, we then obtain microscopic details from fluorescence experiments. Using the coumarin probes with varying hydrophobicities shown in Chart 1, our fluorescence spectra and lifetimes report on both wet and dry PPO, the external aqueous phase (not excluding PEO), and interfacial regions.

Several 7-aminocoumarin fluorophores display properties that make these molecules useful for dynamic probing of condensed phase environments. For example, coumarins are strongly solvatochromic and thus are very sensitive indicators of solvent polarity. The cause of the strong solvatochromism is the large positive change in dipole moment from the  $S_0$  to  $S_1$  state.<sup>67–70</sup> Because of this,

coumarins have been used quite extensively to study solvent–solute reorganization via time-dependent fluorescence Stokes shift (TDFSS).<sup>40,71</sup> The three coumarin molecules used in this study are also relatively rigid, which makes them good probes of microviscosity using the fluorescence anisotropy technique.<sup>41</sup>

In the present study, we are able to selectively probe different regions of aqueous PEO–PPO–PEO triblock copolymer by judicious choice of a very hydrophobic (C153), a hydrophobic (C102), or a relatively hydrophilic (C343<sup>−</sup>/Na<sup>+</sup>) coumarin fluorescent probe molecule (see Chart 1). Figure 2 is a schematic model for how the three coumarins may partition between the different molecular environments in the triblock copolymer micelles. The most hydrophobic C153 is localized in the PPO core, with the C343<sup>−</sup> sodium salt localized in the water phase outside the micelles, and the distribution of C102 spans the hydrophobic PPO core and the PEO corona domains.

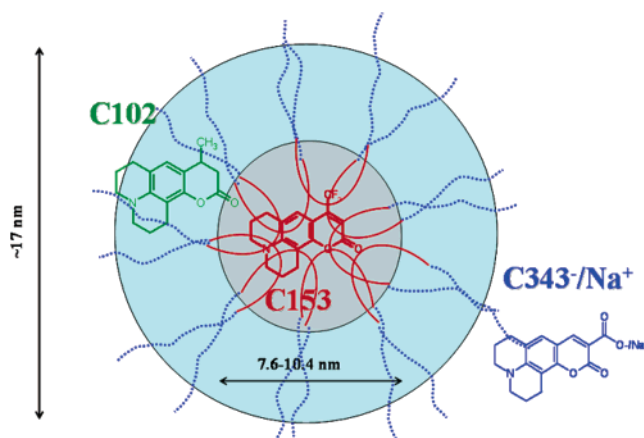


**Figure 2.** Schematic of an F88 micelle interior with C153 in PPO, C102 in PEO, and C343<sup>−</sup>/Na<sup>+</sup> in aqueous domains. Micellar dimensions are taken from ref 16.

## Experimental Section

**Materials.** Pharmaceutical grade poly(ethylene oxide)<sub>109</sub>–poly(propylene oxide)<sub>41</sub>–poly(ethylene oxide)<sub>109</sub> samples were a gift from BASF (Pluronic F88) and were used as received. Fluka Nanopure water was used to dissolve all polymer samples. Laser grade C153 and C102 from Kodak were used as received. Laser grade C343 was obtained from Acros Organics as the free acid and was converted to the sodium carboxylate form by addition of 1.1 equiv of NaOH in methanol. The crystalline C343<sup>−</sup>/Na<sup>+</sup> was recovered after evaporation of the methanol. Polymer solutions were prepared using 0.05 or 0.25 g of Pluronic F88 per 1.0 mL of Nanopure water, for 5 and 25 w/v% solutions, respectively. Solutions were magnetically stirred at room temperature in a sealed container for 12–24 h to fully dissolve the Pluronic F88. Fluorescence samples were made fresh before the experiments.

- (50) Shirota, H.; Horie, K. *J. Phys. Chem. B* **1999**, *103*, 1437.  
 (51) Corbeil, E. M.; Riter, R. E.; Levinger, N. E. *J. Phys. Chem. B* **2004**, *108*, 10777.  
 (52) Sarkar, N.; Datta, A.; Das, S.; Bhattacharyya, K. *J. Phys. Chem. B* **1996**, *100*, 15483.  
 (53) Corbeil, E. M.; Levinger, N. E. *Langmuir* **2003**, *19*, 7264.  
 (54) Pal, S. K.; Sukul, D.; Mandal, D.; Sen, S.; Bhattacharyya, K. *J. Phys. Chem. B* **2000**, *104*, 2613.  
 (55) Changenet-Barret, P.; Choma, C. T.; Gooding, E. F.; DeGrado, W. F.; Hochstrasser, R. M. *J. Phys. Chem. B* **2000**, *104*, 9322.  
 (56) Vajda, S.; Jimenez, R.; Rosenthal, S. J.; Fidler, V.; Fleming, G. R.; Castner, E. W. *J. Chem. Soc., Faraday Trans.* **1995**, *91*, 867.  
 (57) Bart, E.; Meltsin, A.; Huppert, D. *J. Phys. Chem.* **1994**, *98*, 3295.  
 (58) Das, K.; Sarkar, N.; Das, S.; Datta, A.; Bhattacharyya, K. *Chem. Phys. Lett.* **1996**, *249*, 323.  
 (59) Frauchiger, L.; Shirota, H.; Urich, K. E.; Castner, E. W., Jr. *J. Phys. Chem. B* **2002**, *106*, 7463.  
 (60) Karmakar, R.; Samanta, A. *J. Phys. Chem. A* **2002**, *106*, 4447.  
 (61) Chakrabarty, D.; Harza, P.; Chakraborty, A.; Seth, D.; Sarkar, N. *Chem. Phys. Lett.* **2003**, *381*, 697.  
 (62) Arzhantsev, S.; Ito, N.; Heitz, M.; Maroncelli, M. *Chem. Phys. Lett.* **2003**, *381*, 278.  
 (63) Chowdhury, P. K.; Halder, M.; Sanders, L.; Calhoun, T.; Anderson, J. L.; Armstrong, D. W.; Song, X.; Petrich, J. W. *J. Phys. Chem. B* **2004**, *108*, 10245.  
 (64) Ito, N.; Arzhantsev, S.; Heitz, M.; Maroncelli, M. *J. Phys. Chem. B* **2004**, *108*, 5771.  
 (65) Shirota, H.; Tamoto, Y.; Segawa, H. *J. Phys. Chem. A* **2004**, *108*, 3244.  
 (66) Malmsten, M.; Lindman, B. *Macromolecules* **1993**, *26*, 1282.  
 (67) Chowdhury, A.; Locknar, S. A.; Premvardhan, L. L.; Peteanu, L. A. *J. Phys. Chem. A* **1999**, *103*, 9614.  
 (68) Matyushov, D. V.; Newton, M. D. *J. Phys. Chem. A* **2001**, *105*, 8516.

- (69) Cave, R. J.; Burke, K.; Castner, E. W., Jr. *J. Phys. Chem. B* **2002**, *106*, 9294.  
 (70) Cave, R. J.; Castner, E. W., Jr. *J. Phys. Chem. B* **2002**, *106*, 12117.  
 (71) Barbara, P. F.; Jarzaba, W. *Adv. Photochem.* **1990**, *15*, 1.

**Viscometry.** Viscometry measurements were performed using a Cambridge Applied System model ViscoLab 4100 automated viscometer (SPL480 sensor with thermal jacket) for solutions of Pluronic F88. The viscometer contains two magnetic coils inside a stainless steel body to drive a piston back and forth through the fluid. The time required to move the piston a fixed distance is related to the shear viscosity of the fluid. The viscometer unit was cleaned thoroughly with acetone and dried before measurements. The viscometer temperature was controlled between 4 and 80 °C using a Lauda refrigerating circulator (model RMT-6) accurate to 0.1 °C. The measurements were not taken until the temperature had stabilized to a precision of better than 0.1 °C. Instrument specifications state measurement accuracies of <1% for shear viscosities ranging from 0.2 to 10 000 cP, using a series of 5 calibrated stainless steel pistons of varying diameters.

**Steady-State Spectroscopy.** Steady-state fluorescence excitation and emission spectra were recorded on a Spex FluoroMax-3 instrument with photon counting detection using 1 nm spectral resolution. Sample temperatures were controlled to a precision of <0.1 °C over the range of 2.5–90 °C using a thermoelectrically regulated sample holder. Samples were allowed to equilibrate for at least 10 min after a change in temperature prior to data collection. Peak spectral wavelengths are determined by fitting the spectrum full width at 90% of maximum to a Gaussian function.

**Time-Resolved Emission Spectroscopy.** Details of the time-correlated single photon counting (TCSPC) instrument have been described previously.<sup>72,73</sup> Recently, a Becker and Hickl TCSPC data acquisition board, model SPC-630, replaced the older NIM-style electronics. A quartz depolarizer (Optics for Research) is placed directly in front of the spectrometer entrance slit. The depolarizer eliminates polarization bias arising from the spectrometer grating. In addition, a Glan-Laser polarizer is placed in front of the sample to define vertical polarization for excitation, with a matched polarizer used as an analyzer for the emission set at the magic angle (54.7° from vertical) for fluorescence lifetime decays devoid of contributions from the orientational response of the chromophore.<sup>41</sup> When the orientational information is collected and analyzed, one obtains an effective local microviscosity from the time scale for probe molecule reorientation.<sup>74</sup>

For each coumarin probe, fluorescence decays were measured at different excitation (400–440 nm) and emission (478–550 nm) wavelengths depending on the concentrations and temperatures of the copolymer sample. This wavelength selection is done to minimize distortions to the fluorescence lifetime transient that inevitably arise in the short time portions of transients of any solvatochromic probe when placed in a dynamically evolving polar medium,<sup>40,71</sup> such as the aqueous Pluronic F88 samples. The solvent reorganization about the larger polarity excited state causes rapidly evolving fluorescence dynamics that we will make substantial use of in future work. We select the emission wavelength for the fluorescence transients to maximize the contribution from the fluorescence lifetime while minimizing effects from the spectral evolution that results from dynamic solvent reorganization.

The TCSPC transients were acquired so that the peak channel contained up to 65 535 ( $2^{16}-1$ ) fluorescence counts. Time windows of 60 or 70 ns were used to obtain the complete rise and decay profile of the fluorescent transient. Each transient was acquired with 4096 data points for a resolution of 14.6 or 17.1 ps/channel. Instrument response profiles for the TCSPC instrument were obtained by scattering excitation light from an aqueous suspension of nondairy creamer. The instrument response was typically ~40 ps fwhm. Coumarin concentrations were adjusted to obtain absorbance values in the range from 0.1 to 0.3 at the excitation wavelength (10 mm path). Transients were collected for temperatures in the range from 2.5 to 90 ± 0.1 °C using a Quantum Northwest TLC-50/100 thermoelectric temperature controller for the sample holder.

Fluorescence transients were analyzed using a multiple exponential decay model function,  $I(t)$ , given by eq 1.

$$I(t) = \sum_{i=1}^n \alpha_i \exp(-t/\tau_i) \quad (1)$$

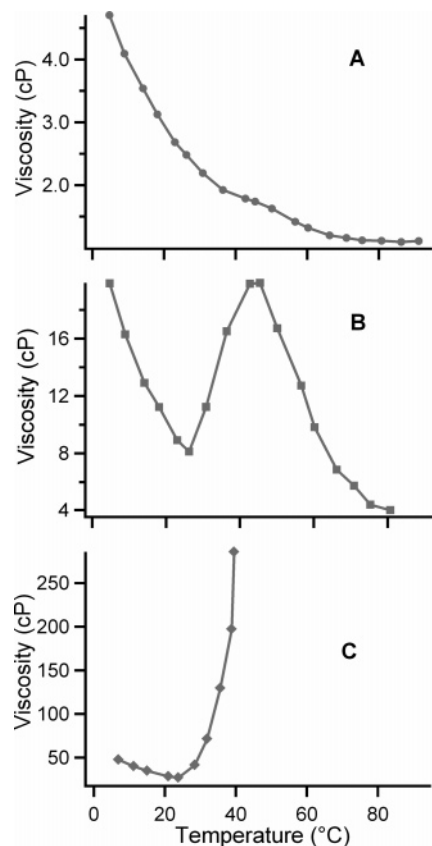


**Figure 3.** Viscosity vs temperature plots for aqueous F88 solutions: (A) 5 w/v%; (B) 15 w/v%; (C) 25 w/v%.

where  $\alpha_i$  and  $\tau_i$  are the amplitude and time component, respectively, of the  $i$ th decay.<sup>75,76</sup> Intensity-averaged decay lifetimes were calculated via the following equation:<sup>75,76</sup>

$$\langle \tau \rangle = \frac{\sum_{i=1}^n \alpha_i \tau_i^2}{\sum_{i=1}^n \alpha_i \tau_i} \quad (2)$$

Fluorescence lifetimes were fit to multiple exponential decay models using forward Fourier transform convolution between fluorescence transients and measured temporal instrument response functions, followed by convolute-and-compare nonlinear least-squares fitting, using macro functions written in IgorPro software (Wavemetrics, Inc., version 4.09A).<sup>77</sup> The criteria for a good fit were based upon a reduced chi-squared ( $\chi^2$ ) value close to unity as well as weighted residuals having a random distribution about zero. Though the decay of the fluorescent excited state is dominated by the intrinsic lifetime of the probe, double- and triple-exponential decay laws are used to obtain the best fits, to account for the unavoidable minority decay components that arise from the time-dependent fluorescence Stokes shift.<sup>40,78</sup>

## Results

The shear viscosities of Pluronic F88 solutions measured as a function of temperature are shown in Figure 3. Figure

(72) Shirota, H.; Castner, E. W., Jr. *J. Chem. Phys.* **2000**, *112*, 2367.  
(73) Sun, Y.; Castner, E. W.; Lawson, C. L.; Falkowski, P. G. *FEBS Lett.* **2004**, *570*, 175.

(74) Jeon, S.; Bae, S. C.; Turner, J.; Granick, S. *Polymer* **2002**, *43*, 4651.

(75) Lakowicz, J. R. *Principles of Fluorescence Spectroscopy*, 2nd ed.; Kluwer Academic: New York, 1999.

(76) Valeur, B. *Molecular Fluorescence, An Introduction: Principles and Applications*, 1st ed.; Wiley-VCH: Weinheim, 2001.

(77) IgorPro, 4.09A ed.; Wavemetrics, Inc.: Lake Oswego, OR, 2003.

(78) Maroncelli, M.; Fleming, G. R. *J. Chem. Phys.* **1987**, *86*, 6221.

3A shows the viscosity results for 5 w/v% aqueous F88 solutions over the temperature range from 5 to 90 °C. For this 5 w/v% solution, the viscosity decays smoothly with increasing temperature in the ranges from about 5 to 35 °C and 55 to 90 °C, but there is a pronounced hump in the curve at about 45 °C that is noticeably above the measured errors of <1%. On increasing the A-B-A triblock copolymer concentration to 15 w/v%, the hump in the viscosity/temperature plot changes into a peak at 45 °C following a local minimum at 26 °C. Both the 5 and 15 w/v% solutions are known to form micelles with increasing temperature and to display unimer behavior for temperatures below the critical micelle concentration (cmc). On increasing the concentration to 25 w/v% Pluronic F88, the viscosity/temperature plot shows shear viscosity decreasing with temperature with an inflection point at 24 °C. The viscosity then begins rising with increasing temperature, exhibiting an exponential growth in viscosity starting at 39.5 °C, which is close to the macroscopic critical gel temperature (cgT) observed near 40 °C.

Critical micelle temperatures were determined by DSC (see Supporting Information for data) for both 5 and 25 w/v% concentrations. The cmT is obtained from the DSC plot at the onset of heat flow.<sup>26,28,79,80</sup> We determined the onset temperature for the microphase transition by taking the numerical first derivative of the DSC temperature scans. As with previous work, there is a concentration dependence on the cmT and this is born out in our experiments. More specifically, at the higher copolymer concentrations the cmT is driven down to lower temperatures compared to lower copolymer concentrations. Our DSC results show that for 25 w/v% the cmT is 20.5 °C while for 5 w/v% the cmT is at 35 °C. The dynamic light scattering results are qualitatively consistent with our DSC determination of the cmT and are presented in the Supporting Information.

Analysis of the fluorescence excitation and emission spectra is accomplished by plotting peak energy (units in  $\text{cm}^{-1}$ ) shift for spectra versus temperature; these plots are given in Figures 4 and 5. The spectra are presented in the Supporting Information. Figure 4 shows excitation (upper graph) and emission spectra (lower graph) for 5 w/v% aqueous F88 copolymer solutions. Both C153 and C102 show a dramatic increase to higher energies in excitation and emission spectra with temperature. Most of the spectral shift occurs through the microphase transition from unimers to micelles. The C153 excitation spectra display a frequency shift of  $960 \text{ cm}^{-1}$  to higher energy with increasing temperature over the microphase transition, while C102 shifts to higher energies by  $770 \text{ cm}^{-1}$  but at a temperature that is about 4 °C higher. C153 also displays a similar blue shift of  $700 \text{ cm}^{-1}$  in the emission spectra versus temperature. The C102 peak emission energy shifts by  $685 \text{ cm}^{-1}$ , and the transition is also shifted by 4 °C relative to C153. The C343 anion excitation peak shifts almost monotonically to higher energy by  $495 \text{ cm}^{-1}$ . However, C343/ $\text{Na}^+$  emission spectra show little variation ( $33 \text{ cm}^{-1}$ ) with increasing temperature.

Plots of the fluorescence excitation and emission peak energy versus temperature in Figure 5 for 25 w/v% F88 show an abrupt blue shift with increasing temperature for both C153 and C102. This behavior is similar to that observed for the lower concentration copolymer solution. With increasing temperature, the excitation spectra for C153 and C102 shift to the blue by  $1136$  and  $1154 \text{ cm}^{-1}$ ,

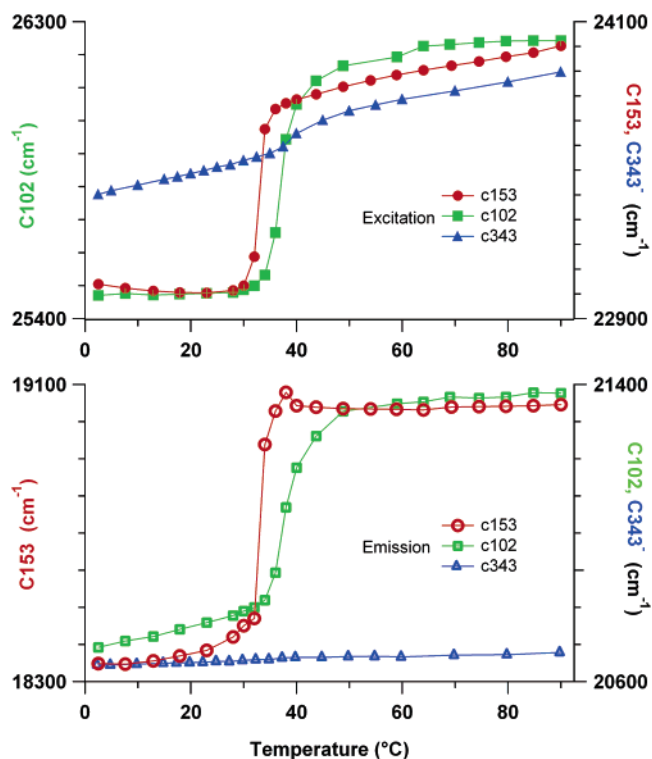


**Figure 4.** Fluorescence spectral shifts vs temperature for 5 w/v% aqueous F88 solutions for coumarins 153, 102, and 343<sup>-</sup>. The top graph shows the fluorescence excitation spectral shifts, and the bottom graph the emission shifts. Shifts are plotted in reduced frequency units, with  $100 \text{ cm}^{-1}$  spacing between adjacent ticks on the vertical axis.

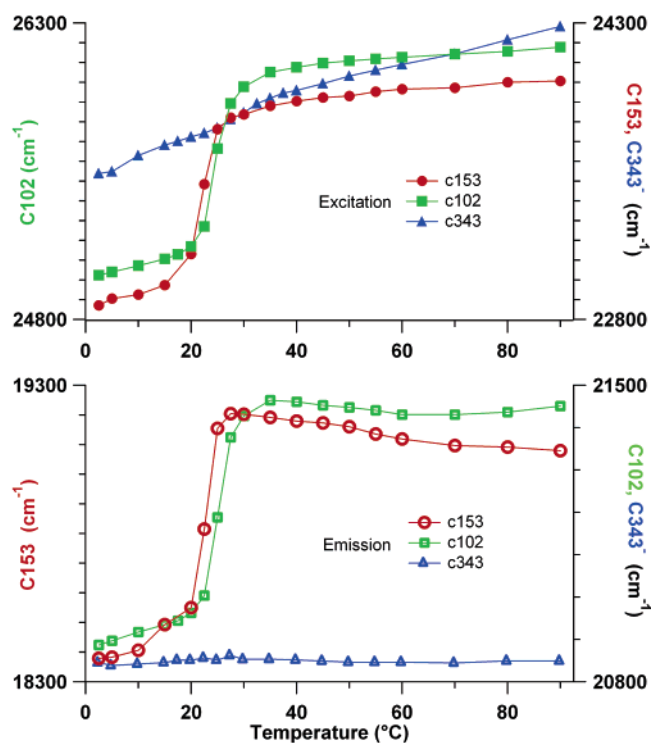


**Figure 5.** Fluorescence spectral shifts vs temperature for 25 w/v% aqueous F88 solutions for coumarins 153, 102, and 343<sup>-</sup>. The top graph shows the fluorescence excitation spectral shifts, and the bottom graph the emission shifts. Shifts are plotted in reduced frequency units, with  $100 \text{ cm}^{-1}$  spacing between adjacent ticks on the vertical axis.

(79) Alexandridis, P.; Holzwarth, J. F. *Langmuir* **1997**, *13*, 6074.  
 (80) Anderson, B. C.; Cox, S. M.; Ambardekar, A. V.; Mallapragada, S. K. *J. Pharm. Sci.* **2002**, *91*, 180.

respectively, while a  $700 \text{ cm}^{-1}$  energy peak blue shift is observed in the emission spectra for C153 with C102

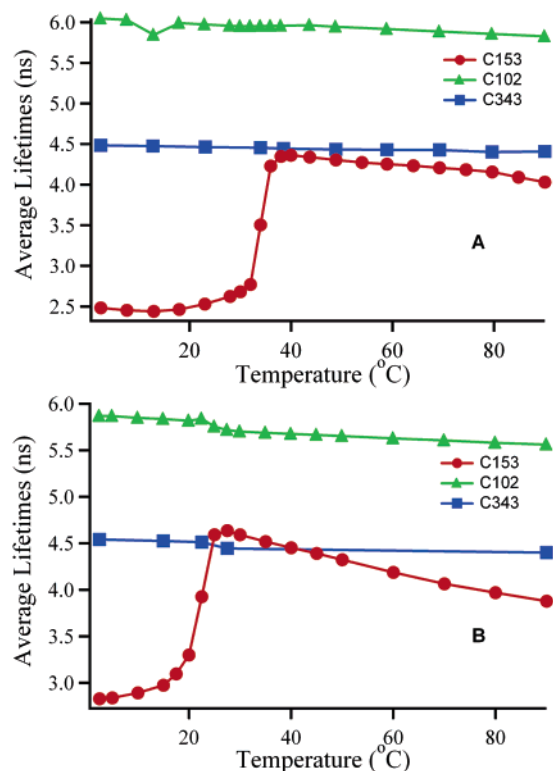


**Figure 6.** Plot of intensity-averaged lifetimes for C153, C102, and C343 versus temperature: (A) 5 w/v% aqueous F88; (B) 25 w/v% aqueous F88.

shifting to the blue by  $564\text{ cm}^{-1}$ . However, the C102 spectral peak shifts at a temperature approximately  $2.5\text{ }^{\circ}\text{C}$  higher than for C153. Because the sample temperature was controlled to  $<0.1\text{ }^{\circ}\text{C}$  and a temperature equilibration time of at least 10 min was used following sample temperature changes, the difference between C153 and C102 emission and excitation spectral shifts in both concentrations appears to be quite significant. C343 $^{-}/\text{Na}^{+}$ , on the other hand, exhibits very little emission shift in either concentration as a function of temperature but does blue shift monotonically  $744\text{ cm}^{-1}$  in the excitation spectra.

Figure 6 plots intensity-averaged lifetimes ( $\langle\tau\rangle$ ) (calculated from eq 2) versus temperature, for each of the three coumarins studied, in both 5 and 25 w/v% aqueous F88 samples. For C102 and C343 $^{-}/\text{Na}^{+}$ , there is a small overall decrease in emission lifetime with increasing temperature for both F88 triblock concentrations. The trends for C102 and C343 $^{-}/\text{Na}^{+}$  lifetimes versus temperature generally follow an Arrhenius trend. The decrease in lifetime for C102 and C343 $^{-}/\text{Na}^{+}$  through the  $2.5\text{--}90\text{ }^{\circ}\text{C}$  temperature range is only a few percent for both 5 and 25 w/v% aqueous F88 solutions.

In contrast to the results for C102 and C343 $^{-}/\text{Na}^{+}$ , the C153 intensity-averaged emission lifetime ( $\langle\tau\rangle$ ) shows a significant increase with increasing temperature near the microphase transition, as shown in Figure 6. For the 5 w/v% aqueous F88 concentration, the C153 lifetime decreases slightly from 2.5 to 15  $^{\circ}\text{C}$  but the C153 lifetime in 25 w/v% aqueous F88 solution increases only slightly from 2.5 to 17.5  $^{\circ}\text{C}$ . In the 5 w/v% aqueous F88 solution, the intensity-averaged emission lifetime ( $\langle\tau\rangle$ ) jumps from a minimum of 2.4 ns at 13  $^{\circ}\text{C}$  to a maximum of 4.4 ns at 40  $^{\circ}\text{C}$ . For the 25 w/v% copolymer solution, the C153 lifetime ( $\langle\tau\rangle$ ) increases sharply from 2.8 to 4.6 ns across the unimer to micelle microphase transition for the temperature range from 20 to 27.5  $^{\circ}\text{C}$ . It is also apparent that the temperature at which the dramatic change in lifetime

**Table 1. Critical Micelle Temperatures for 5 and 25 w/v% Aqueous Pluronic F88 Solutions**

method	cmT ( $^{\circ}\text{C}$ ),	
	5 w/v% aq F88	25 w/v% aq F88
DPH solubility <sup>a</sup>	30.5	
DSC	$35 \pm 1$	$20.5 \pm 1$
C153 excitation shift	$34 \pm 1$	$22.5 \pm 1$
C153 emission shift	$34 \pm 1$	$22.5 \pm 1$
C153 fluorescence lifetime	$34 \pm 1$	$22.5 \pm 1$

<sup>a</sup> As measured by increase in absorbance of diphenylhexatriene vs temperature; ref 27.

is observed occurs at a higher temperature in the 5 w/v% than in the 25 w/v% solution. The transition temperatures from the plots of  $\langle\tau\rangle$  vs temperature are strongly correlated with those observed in our DSC measurements, which show an onset of heat flow for 25 w/v% aqueous F88 at  $\sim 20\text{ }^{\circ}\text{C}$ , and at  $\sim 35\text{ }^{\circ}\text{C}$  for the lower polymer concentration. This onset in observed heat flow has been attributed to dehydration of the hydrophobic PPO core.<sup>26,28,79,80</sup> The change in fluorescence lifetime for C153 is also strongly correlated to the micellization transition observed in our DLS experiments.

Critical temperatures for the unimer to micelle microphase transitions for aqueous F88 solutions are summarized in Table 1. Fluorescence data are reported only for coumarin 153, because only this dye resides uniquely in the micelle core. Good qualitative agreement is found with the earlier critical micelle temperature reported by Alexandridis et al. using the dye solubilization method with diphenylhexatriene.<sup>27</sup>

## Discussion

PEO–PPO–PEO triblocks have been well characterized in the literature, and in general our results are in good agreement with previous studies done using DLS, DSC, and viscometry methods. Figure 3 shows a peak in viscosity versus temperature at approximately  $45\text{ }^{\circ}\text{C}$  for both 5 and 15 w/v% polymer. For the 25 w/v% concentration (the concentration that forms hydrogels), a steep increase in shear viscosity is observed at around  $40\text{ }^{\circ}\text{C}$ . This macroscopic change in viscosity for all three concentrations must result from microscopic entanglements between micelles (PEO interpenetration between micelles) and hence gives an estimate of the gelation temperature.<sup>14</sup> However, the total micelle volume fraction is too small in the lower concentration solutions to form a cubic packed lattice. It is important to note that the viscosity measurements are most sensitive to the gelation transition but are not as sensitive to the unimer to micelle microphase transition that shows a substantial heat flow.

The three coumarin chromophores used in this study were chosen because they have substantial variations in hydrophobicity while sharing a similar rigid molecular framework and similar molecular volume. Because of their differences in relative solubilities, each of these three coumarins probes a different microenvironment, and their emission spectra and dynamics provide information on each of their respective regions in these aggregates. The C343 anion is quite hydrophilic and localizes in highly polar, water rich environments, e.g., bulk water or fully hydrated PEO. C102 is relatively hydrophobic and is likely spanning the PEO and PPO regions, but since it is also slightly water soluble it also may sample the purely aqueous environment, though the fraction of C102 in bulk water is probably small. C153 is water insoluble resulting from the extreme hydrophobicity of the  $-\text{CF}_3$  group, so C153 must be present only in the most hydrophobic

regions, namely, the PPO cores of the triblock copolymer aggregates.

Solvatochromic solutes such as the three coumarins used in this work have fluorescence excitation and emission spectra that are strongly dependent on the polarity of the surrounding medium. As the dipolar nature of the environment shifts from polar to nonpolar, the emission spectrum undergoes a hypsochromic shift since the difference between excited- and ground-state dipole moments is positive, or  $|\mu_e| - |\mu_g| > 0$ . Hence, the shift to shorter wavelength in the steady-state excitation and emission spectra (see Figures 4 and 5) with increasing temperature for both C102 and C153 is a manifestation of the decrease in the local solvent polarity of the environment. Interestingly, the onset of a blue shift with increasing temperature for both probe molecules is roughly correlated with the micellization transition in the F88 solutions based on DSC measurements. It has been shown quite clearly from previous work using SANS<sup>16,23,24</sup> and NMR<sup>81</sup> that the hydrophobic core is dehydrated upon micellization. The exclusion of water and burying of the hydrophobic PPO block in the micelle cores lead to a significant reduction in local solvent polarity. The lack of an abrupt steady-state emission shift for C343<sup>-</sup>/Na<sup>+</sup> with increasing temperature indicates the polarity of its microenvironment must not be changing much through the microphase transition. However, it does appear that the fluorescence excitation spectra of C343<sup>-</sup>/Na<sup>+</sup> are slightly sensitive to the micellization microphase transition, displaying an  $\sim 130$  cm<sup>-1</sup> (2 nm) hypsochromic shift. Temperature-dependent control spectra measured for neutral and salt forms of C343 in water show that the overall blue shift (apart from the abrupt approximately 130 cm<sup>-1</sup> change at the microphase transition from unimers to micelles) of the C343 anion in both F88 concentrations appears to be a temperature effect and not one of changing microenvironment.

The spectral shift arising from the unimer-to-micelle microphase transition from either the C102 fluorescence excitation or emission spectral shifts occurs at a higher temperature than for the corresponding experiment with C153. The C102 transition temperature is 4.0 °C higher than for C153 at the 5 w/v% F88 concentration but is only 2.5 °C higher for the 25 w/v% F88 concentration. This is why we infer that the local environment of C102 differs from that of C153 and C343 anion and more likely spans multiple microenvironments. Preliminary analysis of fluorescence anisotropy data using the triumvirate of C153, C102, and C343<sup>-</sup>/Na<sup>+</sup> fluorophores also supports the existence of multiple microenvironments for C102 at precisely the same microphase transition temperatures.<sup>82</sup>

The work of Jones et al. has demonstrated the sensitivity of C153 to water that is manifested in a greatly reduced fluorescence quantum yield relative to other organic solvents.<sup>83</sup> A variation in C153 fluorescence lifetime with polarity was also reported by Shirota and Castner.<sup>72</sup> They observed a decrease in fluorescence lifetime as a function of increasing water content in binary solutions of 1-propanol/water. Gas-phase electronic structure calculations performed on C153 showed a great sensitivity to the addition of 1, 2, and 3 water molecules.<sup>69,70,84,85</sup> In general,

much of the spectral sensitivity of 7-aminocoumarins results from the dramatic changes that occur when a protic solvent donates a ground-state hydrogen bond to the coumarin carbonyl oxygen.<sup>86,87</sup> Nibbering and co-workers have demonstrated that weaker H-bond donating solvents such as chloroform and phenol show an excited-state photodissociation of the solvent-donor hydrogen-bond to C102.<sup>88,89</sup> Despite the complexities found for 7-aminocoumarins in terms of H-bonding response, careful studies of the transition dipole matrix elements for absorption and emission of several coumarins have been found to be nearly independent of solvent, whether the solvent is protic or not.<sup>87,90</sup> Overall, the approximately 700 cm<sup>-1</sup> shifts in C153 and C102 emission spectra are assigned to result from the disappearance of H-bonded water as micellization and gelation proceed with increasing temperature.

As indicated above, our preliminary fluorescence anisotropy dynamics measurements show substantially hindered reorientational motion (or enhanced microviscosity) upon micellization relative to the unimer solution.<sup>82</sup> We conclude that the increase in fluorescence lifetime for C153 with increasing temperature results more from the loss of hydrogen-bond donation resulting from dehydration of the PPO core, rather than from the presence of a more rigid environment.

## Conclusions

Three coumarin probes of varying hydrophobicity were used to independently probe spectral dynamics in different regions of aqueous Pluronic F88 triblock copolymer solutions. Unimer-to-micelle microphase transition temperatures are obtained for both 5 and 25 w/v% aqueous Pluronic F88 solutions using DSC and DLS. The transition temperatures were found to be  $\sim 35$  and  $\sim 20$ – $25$  °C, respectively. Viscometry measurements yield an approximate temperature for gelation of about 40 °C in the 25 w/v% aqueous copolymer solution. For lower concentrations at which there is an insufficient micelle volume fraction to form gels, there nonetheless exist significant microscopic entanglements between micelles, causing a substantial change in the macroscopic viscosity response versus temperature. Steady-state emission and excitation spectral shifts for both C102 and C153 are correlated with dehydration of aqueous PPO hydrophobic regions. Thus these probes are sensitive to the micellization transition, but not to hydrogelation, since the shifts correlate with heat flow (DSC) and light scattering but not macroscopic viscosity. The temperature-dependent steady-state fluorescence spectral shift and increase in emission lifetime for C153 accurately reflect the true micellization temperature because C153 is localized in the triblock copolymer's hydrophobic PPO core. C102 likely spans multiple regions of the aqueous Pluronic F88 micelles and hydrogels, including the hydrophobic PPO core, the wet PEO micellar corona, and perhaps a very small fraction of C102 in bulk water outside the aggregates. Though subtle, the most convincing evidence for this prediction is that the C102 hypsochromic emission shift occurs at a slightly higher temperature than for the C153 shift. Also, preliminary fluorescence anisotropy dynamics show a smaller

(81) Cau, F.; Lacelle, S. *Macromolecules* **1996**, *29*, 170.

(82) Grant, C. D.; Steege, K. E.; DeRitter, M. R.; Castner, E. W. J. In preparation.

(83) Jones, G., II; Jackson, W. R.; Choi, C.-y.; Bergmark, W. R. *J. Phys. Chem.* **1985**, *89*, 294.

(84) Pryor, B. A.; Palmer, P. M.; Andrews, P. M.; Berger, M. B.; Topp, M. R. *J. Phys. Chem. A* **1998**, *102*, 3284.

(85) Pryor, B. A.; Palmer, P. M.; Chen, Y.; Topp, M. R. *Chem. Phys. Lett.* **1999**, *299*, 536.

(86) Moog, R. S.; Bankert, D. L.; Maroncelli, M. *J. Phys. Chem.* **1993**, *97*, 1496.

(87) Moog, R. S.; Davis, W. W.; Ostrowski, S. G.; Wilson, G. L. *Chem. Phys. Lett.* **1999**, *299*, 265.

(88) Nibbering, E. T. J.; Chudoba, C.; Elsaesser, T. *Isr. J. Chem.* **1999**, *39*, 333.

(89) Nibbering, E. T. J.; Tschirschwitz, F.; Chudoba, C.; Elsaesser, T. *J. Phys. Chem. A* **2000**, *104*, 4236.

(90) Lewis, J. E.; Maroncelli, M. *Chem. Phys. Lett.* **1998**, *282*, 197.

and temperature-shifted response for C102 relative to C153.<sup>82</sup> The C153 emission lifetime shows a dramatic increase as the samples are heated above the critical temperature for the microphase transition from unimers to micelles. As indicated by measurements of relative water concentrations in the PPO cores of Pluronic micelles by NMR and neutron scattering contrast, we find that the most probable cause for the C153 lifetime jump is the exclusion of water and not the increase in local friction provided by the self-organized micellar core. C343<sup>-</sup>/Na<sup>+</sup> is localized in bulk water and possibly in wet PEO regions. However, the near absence of emission shift or jump in emission lifetime with increasing temperature indicates that the C343<sup>-</sup>/Na<sup>+</sup> probe is likely present in the bulk water with a small minority component sampling a wet PEO environment.

The results presented using the three coumarins can be generalized to probe multiple environments in many other complex systems. As stated before, A-B-A triblock copolymers based on PEO-PPO-PEO can form as many as nine different microphases.<sup>11</sup> We have shown that we can probe regions of different hydrophobicity by careful selection of an appropriate fluorescence probe molecule. Other diblock (A-B) and triblock (A-B-A and A-B-C) copolymers can be studied using the same fluorescence methods we present here. In addition, the dynamics of hydrophobic pockets of protein systems could be compared with those of protein surfaces and bulk aqueous phases. More detailed information about confined systems, including porous nanomaterials such as zeolites and sol-gel glasses, can be obtained using a good choice of chromophore molecule. Drug encapsulation and delivery systems beyond the PEO-PPO-PEO system we have studied in this report can be characterized in this way. For example, polymeric drug delivery vehicles such as amphiphilic starlike macromolecules (ASMs) can be

studied in even greater detail by judicious choice of hydrophobic or hydrophilic fluorescent probes.<sup>59</sup> Changes in the effective polarity of the local environment within the aggregate surrounding the fluorescence probe are revealed in the emission spectral shift and emission lifetime experiments such as presented here. In particular, we are characterizing the Pluronic F88 systems discussed here using the three coumarins to probe the local microviscosity using fluorescence anisotropy and studying the dynamics of water-polymer interactions using the time-dependent fluorescence Stokes shift.<sup>82</sup>

**Acknowledgment.** We gratefully acknowledge financial support from the donors of the Petroleum Research Fund (ACS-PRF Grant 38564-AC7) and from the National Science Foundation (NSF-CHE-0239390). We thank BASF (Mount Olive, NJ) for donations of high purity Pluronic F88 and our colleagues Professors Larry Romsted and Ken Breslauer for use of the Particle Sizing Systems NICOMP 380 dynamic light scattering and Perkin-Elmer DSC-7 differential scanning calorimeter instruments, respectively. Karen E. Steege gratefully acknowledges support as an NSF IGERT fellow.

**Supporting Information Available:** The experimental methods and results for the DLS and DSC data discussed above. Complete sets of fluorescence excitation and emission spectra are plotted for each of the three coumarin probes for both F88 solution concentrations. Raw time-correlated single-photon counting transients are plotted for five representative temperatures for each coumarin probe and both F88 concentrations. Tables containing the detailed parameters for the multiexponential fluorescence transient analysis are given for the full set of temperature-dependent data, for each coumarin dye, for both polymer concentrations. This material is available free of charge via the Internet at <http://pubs.acs.org>.

LA047560M